International Journal of Analysis and Applications

A Generalized Schrödinger Equation Involving the Parabolic Law of Nonlinear Refractive Index: Its Sideband Instability, Bifurcation Analysis, and Solitary Waves

K. Hosseini[1,2,3,*], F. Alizadeh[1,2], E. Hincal[1,4], S. Boulaaras[5], M.S. Osman[6], C.K. Chan[7]

[1]*Department of Mathematics, Near East University, Mersin 10, Nicosia, 99138, Turkey*
[2]*Research Center of Applied Mathematics, Khazar University, Baku, Azerbaijan*
[3]*Faculty of Engineering and Natural Sciences, Istanbul Okan University, Istanbul, Turkey*
[4]*Department of Mathematical Sciences, Saveetha School of Engineering, SIMATS, Chennai-602105, Tamilnadu, India*
[5]*Department of Mathematics, College of Science, Qassim University, Buraydah 51452, Saudi Arabia*
[6]*Department of Mathematics, Faculty of Science, Cairo University, Giza 12613, Egypt*
[7]*Faculty of Engineering and Quantity Surveying, INTI International University, 71800 Nilai, Negeri Sembilan, Malaysia*

**Corresponding author:* kamyar_hosseini@yahoo.com

ABSTRACT. Throughout the past few decades, the exploration of mathematical models associated with Earth systems has received substantial scholarly focus. The current paper aims to comprehensively explore a generalized Schrödinger equation involving the parabolic law of nonlinear refractive index under an external potential. Specifically, the governing equation for the sideband instability (SI) is examined in detail to distinguish the effects of cubic and quantic nonlinearities on stable and unstable zones. Further, the bifurcation analysis is theoretically and numerically conducted to locate equilibrium points of the generalized Schrödinger equation and identify its solitary and periodic waves. In the end, the impact of nonlinear effects on the propagation of shock and dark waves modeled by the generalized Schrödinger equation is thoroughly analyzed. In light of the results given in the present paper, an increase in the coefficient of the cubic (quantic) nonlinearity leads to an increase (decrease) in the amplitude of shock and dark waves.

Received Dec. 6, 2025

2020 Mathematics Subject Classification. 35R10; 74J35.

Key words and phrases. generalized Schrödinger equation; parabolic law; sideband instability; bifurcation analysis; shock and dark waves.

https://doi.org/10.28924/2291-8639-24-2026-115

ISSN: 2291-8639

1. Introduction

There are many areas of applied sciences in which nonlinear evolution equations (NLEEs) are found. The Korteweg-de Vries (KdV) equation [1], a model of waves on shallow water surfaces, the Benjamin–Bona–Mahony (BBM) equation [2], a model for the unidirectional propagation of nonlinear dispersive long waves, the Boussinesq equation [3], a model of gravity waves in shallow water, and the nonlinear Schrödinger (NLS) equation [4] for the pulse propagation in optical media, all are well-known NLEEs that have attracted particular interest. In recent decades, extensive research has been conducted on the above NLEEs and their generalizations. Hosseini et al. [5] derived multi-soliton waves of a 3D generalized KdV equation using the simplified Hirota method. Estévez et al. [6] applied the factorization method to construct traveling waves of a generalized BBM equation. Alquran and Alhami [7] found bidirectional bell-shaped waves of a generalized Boussinesq equation using the Kudryashov method. Hosseini et al. [8] employed the ansatz method to establish the Gaussian solitary wave of a generalized NLS equation.

Sideband instability is one of the most common phenomena that shows the features of the excited localized modes [9]. The SI is distinguished by a rapidly increasing amplitude of plane waves subject to tiny perturbations, where nonlinear and dispersion expressions interact [9]. The subject of a considerable number of recent studies is sideband instability. For example, Sharma et al. [10] explored the impact of the variation of different effects on the existence of the sideband instability in a nonlinear Schrödinger equation involving an external source. In another research, Xiong and Ren [11] investigated the sideband instability of a coupled Schrödinger equation and discovered that the gain spectrum increases by enhancing the total power P.

In dealing with NLEEs, a main topic to investigate is the bifurcation analysis of their dynamical systems. The bifurcation analysis is crucial in determining equilibrium points of the dynamical system and proving that periodic and solitary waves exist for the governing equation. A great deal of research has been carried out in recent years on NLEEs and their bifurcation analysis. Almusawa et al. [12] conducted complete research on the bifurcation analysis of the modified α equation, confirming the existence of periodic and solitary waves. As a result of their bifurcation analysis for the generalized P-type equation, Jhangeer et al. [13] demonstrated the existence of traveling waves. In another investigation, Raza et al. [14] showed that periodic and solitary waves exist for the Landau–Ginzburg–Higgs equations through the bifurcation analysis. Additional research is found in [15–17].

Solitary waves are wave packets that spread through space without a change in their shape. Such a great feature makes solitary waves an essential tool of data transmission through optical fibers. Due to the governing model, researchers deal with different types of solitary waves, such as shock, dark, and bright waves. In recent decades, a wide range of effective methods, such as the Kudryashov method [18–20], the exponential method [21–23], and the ansatz method [24–26], have been applied to construct solitary waves of NLEEs. Among these, the ansatz method is the

most straightforward and requires the least amount of computational work. Due to its ability to generate solitary waves of NLEEs, such a method has received a lot of interest. Hosseini et al. [27] found solitary waves (bright and dark waves) of a NLS equation of fourth order using the ansatz method. In another study, Alizadeh et al. [28] utilized the ansatz method to derive solitary waves (Shock and bright waves) of a 3D-modified nonlinear wave equation.

The main aim of the current paper is to conduct a full investigation on a generalized Schrödinger equation, i.e.

$$iu_y + \frac{1}{2}(u_{xx} - u_{tt}) + c_1|u|^2u + c_2|u|^4u + u = 0, \tag{1.1}$$

which involves the parabolic law of nonlinear refractive index under an external potential. In Eq. (1.1), c_1 and c_2 are the coefficients of cubic and quantic nonlinearities, while the last term is an external potential. Over the last few years, several studies [29–35] have been conducted on different versions of Eq. (1.1). According to the paper, its motivation is as follows:

- The generalized Schrödinger equation for the sideband instability is examined in depth to distinguish the influence of cubic and quantic expressions on stable and unstable zones;
- To locate equilibrium points of the governing equation and identify its solitary and periodic waves, the bifurcation analysis is theoretically and numerically conducted;
- The impact of nonlinear effects on the propagation of shock and dark waves modeled by the generalized Schrödinger equation is thoroughly analyzed.

2. Model and its sideband instability

Sideband instability can be started by perturbing the solution as follows

$$u(x, y, t) = \left(\sqrt{P} + U(x, y, t)\right) e^{iPt}. \tag{2.1}$$

Through considering Eqs. (1.1) and (2.1) and linearizing, we derive

$$2\left(P\frac{\partial U}{\partial t} - \frac{\partial U}{\partial y}\right) + i\left(\frac{\partial^2 U}{\partial x^2} - \frac{\partial^2 U}{\partial t^2}\right) + i(6P^2c_2 + P^2 + 4Pc_1 + 2)U + 2iP(c_1 + 2Pc_2)\overline{U} = 0, \tag{2.2}$$

where the complex conjugate of U is shown by $\overline{U}$. Now, assume the trial expression

$$U = \lambda_1 e^{i(\mu x + \nu y - \omega t)} + \lambda_2 e^{-i(\mu x + \nu y - \omega t)}, \quad \mu \text{ and } \nu \text{ are wave numbers while } \omega \text{ is the frequency} \tag{2.3}$$

for Eq. (2.2). Setting Eq. (2.3) in Eq. (2.2) along with simplifications yields the system $A\lambda = 0$. For a nontrivial solution, it is essential to have

$$|A| = \begin{vmatrix} A_{11} & A_{12} \\ A_{21} & A_{22} \end{vmatrix} = 0,$$

where

$$A_{11} = -2P^2c_2 - Pc_1,$$

$$A_{12} = -\frac{1}{2}(6c_2 + 1)P^2 - (\omega + 2c_1)P + \frac{1}{2}\mu^2 - \frac{1}{2}\omega^2 - \nu - 1,$$

$$A_{21} = -3P^2c_2 - \frac{1}{2}P^2 + P\omega - 2Pc_1 + \frac{1}{2}\mu^2 - \frac{1}{2}\omega^2 + \nu - 1,$$

$$A_{22} = -2P^2c_2 - Pc_1.$$

Simplification yields

$$-1 - P^2 - \frac{1}{4}P^4 - \frac{1}{4}\mu^4 - \frac{1}{4}\omega^4 - \omega^2 + \mu^2 - 5P^4c_2^2 - 3P^4c_2 - 2P^3c_1 + \frac{1}{2}P^2\mu^2 + \frac{1}{2}P^2\omega^2 - 3P^2c_1^2 + \frac{1}{2}\mu^2\omega^2 + \nu^2 + 3P^2c_2\mu^2 - 8P^3c_1c_2 - 3P^2c_2\omega^2 + 2\omega P\nu + 2Pc_1\mu^2 - 2Pc_1\omega^2 - 4Pc_1 - 6P^2c_2 = 0.$$

Now, solving for μ gives

$$\mu_{1,2} = \pm\sqrt{6P^2c_2 + P^2 + 4Pc_1 + \omega^2 + 2 + 2\sqrt{4P^4c_2^2 + 4P^3c_1c_2 + P^2\omega^2 + P^2c_1^2 + 2\omega P\nu + \nu^2}},$$

$$\mu_{3,4} = \pm\sqrt{6P^2c_2 + P^2 + 4Pc_1 + \omega^2 + 2 - 2\sqrt{4P^4c_2^2 + 4P^3c_1c_2 + P^2\omega^2 + P^2c_1^2 + 2\omega P\nu + \nu^2}}.$$

The steady-state solution becomes unstable when the wave number (μ) has an imaginary part. Accordingly, the condition for the existence of SI is either

$$6P^2c_2 + P^2 + 4Pc_1 + \omega^2 + 2 + 2\sqrt{4P^4c_2^2 + 4P^3c_1c_2 + P^2\omega^2 + P^2c_1^2 + 2\omega P\nu + \nu^2} < 0,$$

or

$$6P^2c_2 + P^2 + 4Pc_1 + \omega^2 + 2 - 2\sqrt{4P^4c_2^2 + 4P^3c_1c_2 + P^2\omega^2 + P^2c_1^2 + 2\omega P\nu + \nu^2} < 0.$$

Finally, the general expression of the SI gain is given by Gain $= 2\,\mathrm{Im}(\mu)$.

In what follows, the impact of cubic and quantic nonlinearities on stable and unstable zones is highlighted by analyzing the gain. To this end, the authors analyze the effect of the cubic nonlinearity on the gain in Figure 1**(a)** when $\nu = -1$, $\omega = -1$, and $P = 1$, and c_1 varies from 1 to 15. It is evident that with increased values of the cubic nonlinearity, stable zones increase. As another study, to assess the impact of the quantic nonlinearity on the gain, the authors plot the gain in Figure 1**(b)** for $\nu = -1$, $\omega = -1$, and $P = 1$ when c_2 changes from 1 to 15. Clearly, stable zones increase with the enhancement of the quantic nonlinearity. In both cases, the amplitude of the plane wave shows a decreasing trend with increasing nonlinear effects.

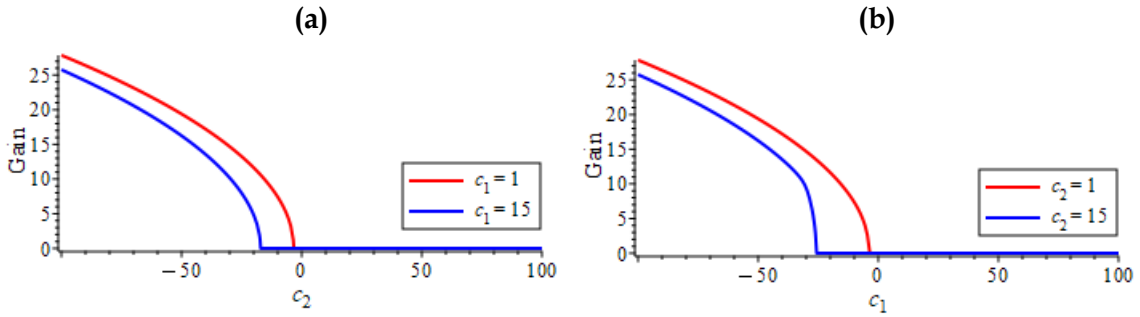

Figure 1: The gain for **(a)** $\nu = -1$, $\omega = -1$, and $P = 1$, when c_1 varies from 1 to 15; **(b)** $\nu = -1$, $\omega = -1$, and $P = 1$ when c_2 changes from 1 to 15

To show the influence of cubic and quantic nonlinearities on stable and unstable zones through a density view, the authors plot the gain in Figure 2 for $\nu = -1$, $\omega = -1$, and $P = 1$. As can be seen in Figure 2, nonlinear effects have a profound impact on stable and unstable zones.

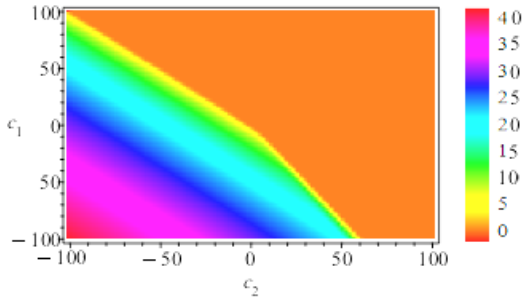

Figure 2: The gain for $\nu = -1$, $\omega = -1$, and $P = 1$

3. Model and its bifurcation analysis

In the present section, the dynamical system corresponding to the governing equation is first presented, and then a bifurcation analysis is conducted to locate its equilibrium points. Such an analysis enables us to ensure the existence of solitary and periodic waves for the governing equation. Through applying the complex field

$$u(x,y,t) = U(\epsilon)e^{i(\lambda_1 x+\lambda_2 y-\nu_2 t)}, \quad \epsilon = \kappa_1 x + \kappa_2 y - \nu_1 t,$$

involving ν_1 as the velocity and ν_2 as the frequency, we find

$$\frac{1}{2}(\kappa_1^2 - \nu_1^2)\frac{d^2U(\epsilon)}{d\epsilon^2} + i(\kappa_1\lambda_1 - \nu_1\nu_2 + \kappa_2)\frac{dU(\epsilon)}{d\epsilon} + \left(-\frac{1}{2}\lambda_1^2 + \frac{1}{2}\nu_2^2 - \lambda_2 + 1\right)U(\epsilon) + c_1U^3(\epsilon) + c_2U^5(\epsilon) = 0. \tag{3.1}$$

From the imaginary part, it is found

$$\kappa_2 = \nu_1\nu_2 - \kappa_1\lambda_1.$$

Accordingly, Eq. (3.1) can be reduced to

$$\frac{1}{2}(\kappa_1^2 - \nu_1^2)\frac{d^2U(\epsilon)}{d\epsilon^2} + \left(-\frac{1}{2}\lambda_1^2 + \frac{1}{2}\nu_2^2 - \lambda_2 + 1\right)U(\epsilon) + c_1U^3(\epsilon) + c_2U^5(\epsilon) = 0. \tag{3.2}$$

It should be mentioned that Eq. (3.2) can be rewritten as follows:

$$\frac{d^2U(\epsilon)}{d\epsilon^2} + \frac{2c_2}{\kappa_1^2-\nu_1^2}U^5(\epsilon) + \frac{2c_1}{\kappa_1^2-\nu_1^2}U^3(\epsilon) + \frac{(-\lambda_1^2+\nu_2^2-2\lambda_2+2)}{\kappa_1^2-\nu_1^2}U(\epsilon) = 0,$$

or

$$\frac{d^2U(\epsilon)}{d\epsilon^2} = \Lambda_1 U(\epsilon)(U^4(\epsilon) + \Lambda_2 U^2(\epsilon) + \Lambda_3), \tag{3.3}$$

where

$$\Lambda_1 = -\frac{2c_2}{\kappa_1^2-\nu_1^2}, \quad \Lambda_2 = \frac{c_1}{c_2}, \quad \Lambda_3 = \frac{-\lambda_1^2+\nu_2^2-2\lambda_2+2}{2c_2}.$$

The dynamical system corresponding to Eq. (3.3) is

$$\begin{cases} \frac{dU}{d\epsilon} = \Omega(U,\Xi) = \Xi, \\ \frac{d\Xi}{d\epsilon} = \Psi(U,\Xi) = \Lambda_1 U(U^4 + \Lambda_2 U^2 + \Lambda_3) = F(U). \end{cases} \tag{3.4}$$

The above system is the Hamiltonian because

$$\frac{\partial \Omega}{\partial U} + \frac{\partial \Psi}{\partial \Xi} = 0,$$

and its Hamiltonian function is given by

$$H(U,\Xi) = \frac{1}{2}\Xi^2 - \frac{1}{6}\Lambda_1 U^6 - \frac{1}{4}\Lambda_1\Lambda_2 U^4 - \frac{1}{2}\Lambda_1\Lambda_3 U^2 = h.$$

The Jacobian of (3.4) is

$$J = \begin{bmatrix} 0 & 1 \\ \Lambda_1(5U^4 + 3\Lambda_2 U^2 + \Lambda_3) & 0 \end{bmatrix},$$

with

$$|J| = -\Lambda_1(5U^4 + 3\Lambda_2 U^2 + \Lambda_3) = -F'(U).$$

Equilibrium points can be found as

$$E_1 = (0,0),\ \ E_{2,3} = \left(\pm\frac{1}{2}\sqrt{-2\left(\Lambda_2 - \sqrt{\Lambda_2^2 - 4\Lambda_3}\right)}, 0\right),\ \ E_{4,5} = \left(\pm\frac{1}{2}\sqrt{-2\left(\Lambda_2 + \sqrt{\Lambda_2^2 - 4\Lambda_3}\right)}, 0\right).$$

I. If $\Theta = (\Lambda_2^2 - 4\Lambda_3) < 0$, then the only equilibrium point is $E_1 = (0,0)$, and we have

$$|J(0,0)| = -F'(0) = -\Lambda_1\Lambda_3.$$

Accordingly, $E_1 = (0,0)$ is a saddle point for $\Lambda_1\Lambda_3 > 0$ and a center point for $\Lambda_1\Lambda_3 < 0$. To see what exactly is happening, we consider the following cases:

Case 1: For $\lambda_1 = 1$, $\kappa_1 = 1$, $\nu_1 = 2$, $\lambda_2 = 1$, $\nu_2 = 2$, $c_1 = 1$, and $c_2 = 1$, we find

$$\Lambda_1 = \frac{2}{3},\ \ \Lambda_2 = 1,\ \ \Lambda_3 = \frac{3}{2},\ \ \Theta = -5 < 0.$$

Since $\Lambda_1\Lambda_3 > 0$, $(0,0)$ represents a saddle point as shown in Figure 3**(a)**.

Case 2: For $\lambda_1 = 1$, $\kappa_1 = 2$, $\nu_1 = 1$, $\lambda_2 = 1$, $\nu_2 = 2$, $c_1 = 1$, and $c_2 = 1$, we discover

$$\Lambda_1 = -\frac{2}{3},\ \ \Lambda_2 = 1,\ \ \Lambda_3 = \frac{3}{2},\ \ \Theta = -5 < 0.$$

Since $\Lambda_1\Lambda_3 < 0$, $(0,0)$ signifies a center point as revealed in Figure 3**(b)**.

II. If $\Theta = (\Lambda_2^2 - 4\Lambda_3) > 0$, then we must have

$$\Lambda_2 - \sqrt{\Theta} < 0 \Rightarrow \Lambda_2 < \sqrt{\Theta},$$

$$\Lambda_2 + \sqrt{\Theta} < 0 \Rightarrow \Lambda_2 < -\sqrt{\Theta}.$$

Therefore, the equilibrium points are

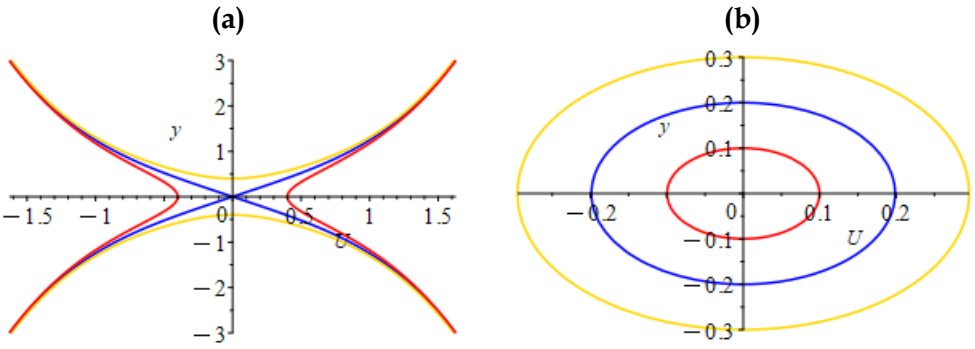

Figure 3: Phase diagrams for **(a)** $\lambda_1 = 1$, $\kappa_1 = 1$, $\nu_1 = 2$, $\lambda_2 = 1$, $\nu_2 = 2$, $c_1 = 1$, and $c_2 = 1$; **(b)** $\lambda_1 = 1$, $\kappa_1 = 2$, $\nu_1 = 1$, $\lambda_2 = 1$, $\nu_2 = 2$, $c_1 = 1$, and $c_2 = 1$

$$E_1 = (0,0),$$
$$E_{2,3} = \left(\pm\frac{1}{2}\sqrt{-2(\Lambda_2 - \sqrt{\Theta})}, 0\right),$$
$$E_{4,5} = \left(\pm\frac{1}{2}\sqrt{-2(\Lambda_2 + \sqrt{\Theta})}, 0\right).$$

It is found that

$$|J(0,0)| = -F'(0) = -\Lambda_1\Lambda_3,$$
$$\left|J\left(\pm\frac{1}{2}\sqrt{-2(\Lambda_2 - \sqrt{\Theta})}, 0\right)\right| = -F'\left(\pm\frac{1}{2}\sqrt{-2(\Lambda_2 - \sqrt{\Theta})}\right) = \Lambda_1\sqrt{\Theta}(\Lambda_2 - \sqrt{\Theta}),$$
$$\left|J\left(\pm\frac{1}{2}\sqrt{-2(\Lambda_2 + \sqrt{\Theta})}, 0\right)\right| = -F'\left(\pm\frac{1}{2}\sqrt{-2(\Lambda_2 + \sqrt{\Theta})}\right) = -\Lambda_1\sqrt{\Theta}(\Lambda_2 + \sqrt{\Theta}).$$

For example, if $\lambda_1 = 2.1$, $\kappa_1 = 2$, $\nu_1 = 1$, $\lambda_2 = 1$, $\nu_2 = 2$, $c_1 = 1.25$, and $c_2 = -1$, we find

$$\Lambda_1 = \frac{2}{3}, \quad \Lambda_2 = -1.25, \quad \Lambda_3 = 0.205, \quad \Theta = 0.7425 > 0,$$

where

$$\Lambda_2 = -1.25 < \sqrt{\Theta} = 0.8616843970, \quad \Lambda_2 = -1.25 < -\sqrt{\Theta} = -0.8616843970.$$

These yield

$$|J(0,0)| = -0.1366666667,$$
$$|J(\pm 0.4406334094,0)| = 0.2230703308,$$
$$|J(\pm 1.027541823,0)| = -1.213070329.$$

Thus, $(0,0)$ and $(\pm 1.027541823,0)$ are saddle points, whereas $(\pm 0.4406334094,0)$ are center points (See Figure 4 **(a)**).

As another example, for the values $\lambda_1 = 2.1$, $\kappa_1 = 1$, $\nu_1 = 2$, $\lambda_2 = 1$, $\nu_2 = 2$, $c_1 = 1.25$, and $c_2 = -1$, we have

$$\Lambda_1 = -\frac{2}{3}, \quad \Lambda_2 = -1.25, \quad \Lambda_3 = 0.205, \quad \Theta = 0.7425 > 0,$$

where

$$\Lambda_2 = -1.25 < \sqrt{\Theta} = 0.8616843970, \quad \Lambda_2 = -1.25 < -\sqrt{\Theta} = -0.8616843970.$$

These yield

$$|J(0,0)| = 0.1366666667,$$
$$|J(\pm 0.4406334094,0)| = -0.2230703308,$$
$$|J(\pm 1.027541823,0)| = 1.213070329.$$

Consequently, $(0,0)$ and $(\pm 1.027541823,0)$ are center points, while $(\pm 0.4406334094,0)$ are saddle points (See Figure 4**(b)**).

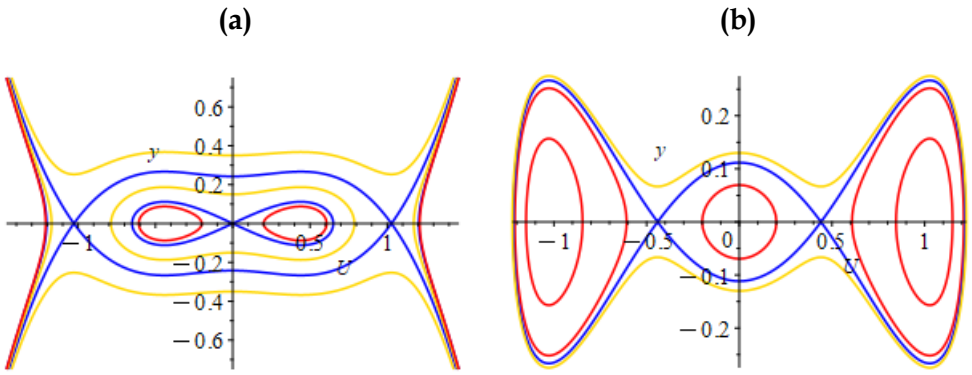

Figure 4: Phase diagrams for **(a)** $\lambda_1 = 2.1$, $\kappa_1 = 2$, $\nu_1 = 1$, $\lambda_2 = 1$, $\nu_2 = 2$, $c_1 = 1.25$, and $c_2 = -1$; **(b)** $\lambda_1 = 2.1$, $\kappa_1 = 1$, $\nu_1 = 2$, $\lambda_2 = 1$, $\nu_2 = 2$, $c_1 = 1.25$, and $c_2 = -1$

III. If $\Theta = \Lambda_2^2 - 4\Lambda_3 = 0$, then the equilibrium points are

$$E_1 = (0,0), \quad E_{2,3} = \left(\pm\frac{1}{2}\sqrt{-2\Lambda_2}, 0\right),$$

where $\Lambda_2 < 0$ and $\Lambda_3 = \frac{1}{4}\Lambda_2^2$.

For example, if $\lambda_1 = 1$, $\kappa_1 = 1$, $\nu_1 = 2$, $\lambda_2 = 2$, $\nu_2 = 1$, $c_1 = 2$, and $c_2 = -1$, we find

$$\Lambda_1 = -\frac{2}{3}, \quad \Lambda_2 = -2, \quad \Lambda_3 = 1, \quad \Theta = 0,$$

where

$$|J(0,0)| = 0.6666666667, \quad |J(\pm 1,0)| = 0.$$

Accordingly, $(0,0)$ is a center point, while $(\pm 1,0)$ are cusp points (See Figure 5**(a)**).

As another case study, if $\lambda_1 = 1$, $\kappa_1 = 2$, $\nu_1 = 1$, $\lambda_2 = 2$, $\nu_2 = 1$, $c_1 = 2$, and $c_2 = -1$, we find

$$\Lambda_1 = \frac{2}{3}, \quad \Lambda_2 = -2, \quad \Lambda_3 = 1, \quad \Theta = 0,$$

and

$$|J(0,0)| = -0.6666666667, \quad |J(\pm 1,0)| = 0.$$

Therefore, $(0,0)$ is a saddle point, whereas $(\pm 1,0)$ are cusp points (See Figure 5**(b)**).

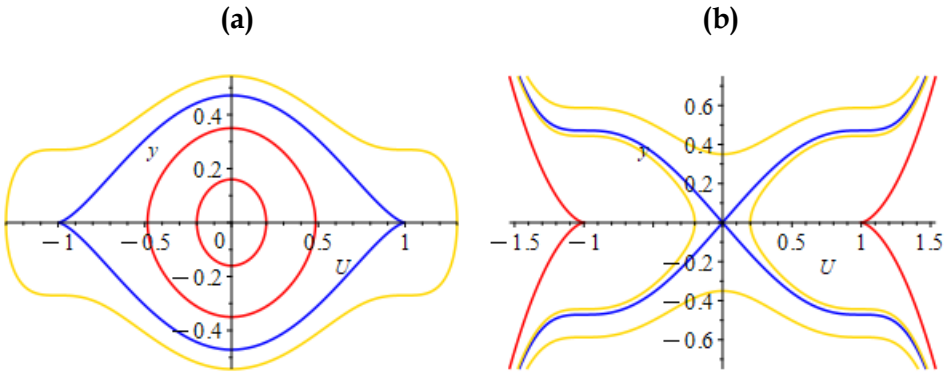

Figure 5: Phase diagrams for **(a)** $\lambda_1 = 1$, $\kappa_1 = 1$, $\nu_1 = 2$, $\lambda_2 = 2$, $\nu_2 = 1$, $c_1 = 2$, and $c_2 = -1$; **(b)** $\lambda_1 = 1$, $\kappa_1 = 2$, $\nu_1 = 1$, $\lambda_2 = 2$, $\nu_2 = 1$, $c_1 = 2$, and $c_2 = -1$

From the bifurcation analysis, it is understood that periodic and solitary waves exist in the governing equation. Accordingly, the next section discusses how to extract such families of waves, particularly shock and dark ones, for the generalized Schrödinger equation. To this end, the authors will employ different ansatzes to find shock and dark waves of the governing equation. Additionally, the impact of nonlinear effects on the propagation of shock and dark waves modeled by the generalized Schrödinger equation is thoroughly analyzed.

4. Model and its solitary waves

In the present section, different ansatzes are utilized to construct shock and dark waves of the generalized Schrödinger equation involving the parabolic law of nonlinear refractive index under an external potential. A thorough analysis is also conducted of the impact of nonlinear effects on the propagation of shock and dark waves modeled by the governing equation.

As the balance number of Eq. (3.2) is not an integer, the authors apply the transformation $U(\epsilon) = \sqrt{\psi(\epsilon)}$. This yields

$$(2\kappa_1^2 - 2\nu_1^2)\psi(\epsilon)\frac{d^2\psi(\epsilon)}{d\epsilon^2} + (-\kappa_1^2 + \nu_1^2)\left(\frac{d\psi(\epsilon)}{d\epsilon}\right)^2 + (-4\lambda_1^2 + 4\nu_2^2 - 8\lambda_2 + 8)\psi^2(\epsilon) + 8c_1\psi^3(\epsilon) + 8c_2\psi^4(\epsilon) = 0, \tag{4.1}$$

with $N = 1$, which is an integer. The process of establishing the first type of solitary waves begins by considering

$$\psi(\epsilon) = A + B\tanh(\epsilon),$$

which A and B are unknowns, and substituting it into the above equation to find the following algebraic system

$$(-\kappa_1^2+\nu_1^2)B^2+8B^4c_2+4(\kappa_1^2-\nu_1^2)B^2=0,$$

$$32AB^3c_2+8B^3c_1+4A(\kappa_1^2-\nu_1^2)B=0,$$

$$-2(-\kappa_1^2+\nu_1^2)B^2+48A^2B^2c_2+24AB^2c_1+4(-\lambda_1^2+\nu_2^2-2\lambda_2+2)B^2-4(\kappa_1^2-\nu_1^2)B^2=0,$$

$$32A^3Bc_2+24A^2Bc_1+8(-\lambda_1^2+\nu_2^2-2\lambda_2+2)AB-4A(\kappa_1^2-\nu_1^2)B=0,$$

$$(-\kappa_1^2+\nu_1^2)B^2+8A^4c_2+8A^3c_1+4(-\lambda_1^2+\nu_2^2-2\lambda_2+2)A^2=0.$$

The solutions for the above system are:

Set 1:

$$A=-\frac{3c_1}{8c_2},\ \ B=-\frac{3c_1}{8c_2},\ \ \kappa_1=\pm\sqrt{-\frac{-8c_2\nu_1^2+3c_1^2}{8c_2}},\ \ \lambda_2=-\frac{8c_2\lambda_1^2-8c_2\nu_2^2+3c_1^2-16c_2}{16c_2}.$$

Therefore, the following solitary waves to the governing equation are derived

$$u_{1,2}(x,t)=\sqrt{-\frac{3c_1}{8c_2}\left(1+\tanh\left(\pm\sqrt{-\frac{-8c_2\nu_1^2+3c_1^2}{8c_2}}x+\left(\nu_1\nu_2\mp\sqrt{-\frac{-8c_2\nu_1^2+3c_1^2}{8c_2}}\lambda_1\right)y-\nu_1t\right)\right)}$$
$$\times e^{i\left(\lambda_1x-\frac{8c_2\lambda_1^2-8c_2\nu_2^2+3c_1^2-16c_2}{16c_2}y-\nu_2t\right)}.$$

Set 2:

$$A=-\frac{3c_1}{8c_2},\ \ B=\frac{3c_1}{8c_2},\ \ \kappa_1=\pm\sqrt{-\frac{-8c_2\nu_1^2+3c_1^2}{8c_2}},\ \ \lambda_2=-\frac{8c_2\lambda_1^2-8c_2\nu_2^2+3c_1^2-16c_2}{16c_2}.$$

Thus, the following solitary waves to the governing equation are acquired

$$u_{3,4}(x,t)=\sqrt{-\frac{3c_1}{8c_2}\left(1-\tanh\left(\pm\sqrt{-\frac{-8c_2\nu_1^2+3c_1^2}{8c_2}}x+\left(\nu_1\nu_2\mp\sqrt{-\frac{-8c_2\nu_1^2+3c_1^2}{8c_2}}\lambda_1\right)y-\nu_1t\right)\right)}$$
$$\times e^{i\left(\lambda_1x-\frac{8c_2\lambda_1^2-8c_2\nu_2^2+3c_1^2-16c_2}{16c_2}y-\nu_2t\right)}.$$

Now, to analyze the impact of the cubic nonlinearity on the propagation of the first solitary wave, it is plotted in Figure 6 for $c_2=1$, $\lambda_1=0.5$, $\nu_1=1$, $\nu_2=1$, $t=0$, and $c_1=1,1.25$. Obviously, the amplitude of the shock wave increases as the coefficient of cubic nonlinearity increases.

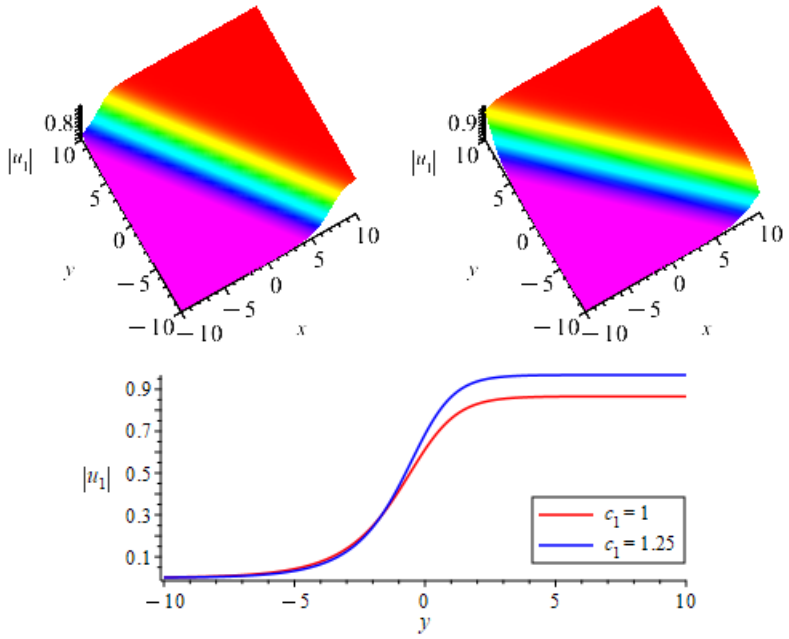

Figure 6: The shock wave in 3D posture for $c_2 = 1$, $\lambda_1 = 0.5$, $\nu_1 = 1$, $\nu_2 = 1$, $t = 0$, and $c_1 = 1{,}1.25$; In 2D posture for $c_2 = 1$, $\lambda_1 = 0.5$, $\nu_1 = 1$, $\nu_2 = 1$, $x = 0$, $t = 0$, and $c_1 = 1{,}1.25$

Figure 7 shows an analysis of the effect of quantic nonlinearity on the propagation of the first solitary wave when $c_1 = 1$, $\lambda_1 = 0.5$, $\nu_1 = 1$, $\nu_2 = 1$, $t = 0$, and $c_2 = 1{,}1.25$. The amplitude of the shock wave shows a decreasing trend with an increasing coefficient of quantic nonlinearity, as shown in Figure 7.

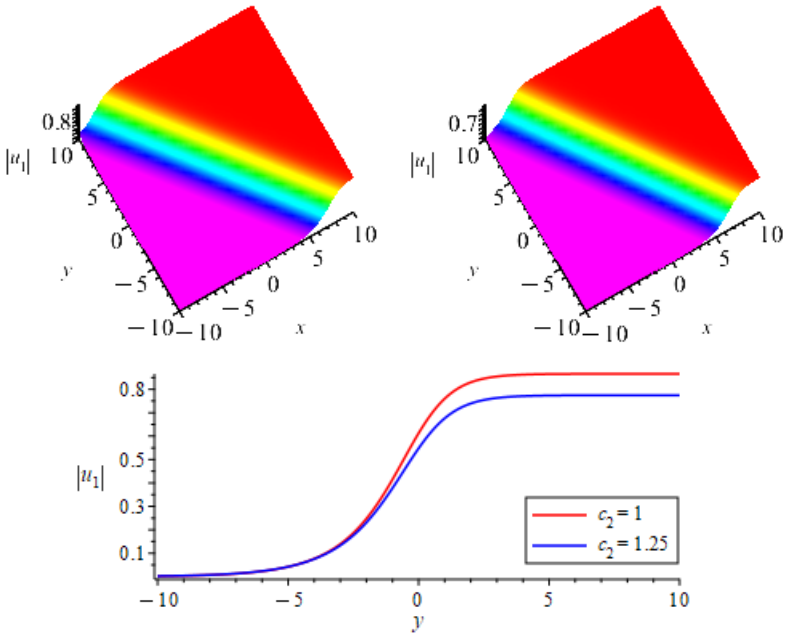

Figure 7: The shock wave in 3D posture for $c_1 = 1$, $\lambda_1 = 0.5$, $\nu_1 = 1$, $\nu_2 = 1$, $t = 0$, and $c_2 = 1{,}1.25$; In 2D posture for $c_1 = 1$, $\lambda_1 = 0.5$, $\nu_1 = 1$, $\nu_2 = 1$, $x = 0$, $t = 0$, and $c_2 = 1{,}1.25$

As the second step in establishing other solitary waves, let us consider

$$\psi(\epsilon) = A + B\,\mathrm{sech}(\epsilon),$$

which A and B are unknowns, and insert it into Eq. (4.1). This results in the following system of algebraic type

$$8c_2B^4 + 3(-\kappa_1^2 + \nu_1^2)B^2 = 0,$$

$$8(4Ac_2 + c_1)B^3 + 4(-\kappa_1^2 + \nu_1^2)AB = 0,$$

$$A^2c_2 + \frac{1}{2}Ac_1 - \frac{1}{48}\nu_1^2 + \frac{1}{12}\nu_2^2 + \frac{1}{48}\kappa_1^2 - \frac{1}{12}\lambda_1^2 - \frac{1}{6}\lambda_2 + \frac{1}{6} = 0,$$

$$A^2c_2 + \frac{3}{4}Ac_1 - \frac{1}{16}\nu_1^2 + \frac{1}{4}\nu_2^2 + \frac{1}{16}\kappa_1^2 - \frac{1}{4}\lambda_1^2 - \frac{1}{2}\lambda_2 + \frac{1}{2} = 0,$$

$$A^2c_2 + Ac_1 + \frac{1}{2}\nu_2^2 - \frac{1}{2}\lambda_1^2 - \lambda_2 + 1 = 0,$$

whose solution is

Set 1:

$$A = -\frac{3c_1}{8c_2},\ B = \frac{3c_1}{8c_2},\ \kappa_1 = \pm\sqrt{-\frac{-8c_2\nu_1^2 - 3c_1^2}{8c_2}},\ \lambda_2 = -\frac{32c_2\lambda_1^2 - 32c_2\nu_2^2 + 15c_1^2 - 64c_2}{64c_2}.$$

Consequently, the following solitary waves to the governing equation are obtained

$$u_{5,6}(x,t) = \sqrt{-\frac{3c_1}{8c_2}\left(1 - \mathrm{sech}\left(\pm\sqrt{-\frac{-8c_2\nu_1^2 - 3c_1^2}{8c_2}}x + \left(\nu_1\nu_2 \mp \sqrt{-\frac{-8c_2\nu_1^2 - 3c_1^2}{8c_2}}\lambda_1\right)y - \nu_1 t\right)\right)}$$
$$\times e^{i\left(\lambda_1 x - \frac{32c_2\lambda_1^2 - 32c_2\nu_2^2 + 15c_1^2 - 64c_2}{64c_2}y - \nu_2 t\right)}.$$

Set 2:

$$A = -\frac{3c_1}{8c_2},\ B = -\frac{3c_1}{8c_2},\ \kappa_1 = \pm\sqrt{-\frac{-8c_2\nu_1^2 - 3c_1^2}{8c_2}},\ \lambda_2 = -\frac{32c_2\lambda_1^2 - 32c_2\nu_2^2 + 15c_1^2 - 64c_2}{64c_2}.$$

Thus, the following solitary waves to the governing equation are constructed

$$u_{7,8}(x,t) = \sqrt{-\frac{3c_1}{8c_2}\left(1 + \mathrm{sech}\left(\pm\sqrt{-\frac{-8c_2\nu_1^2 - 3c_1^2}{8c_2}}x + \left(\nu_1\nu_2 \mp \sqrt{-\frac{-8c_2\nu_1^2 - 3c_1^2}{8c_2}}\lambda_1\right)y - \nu_1 t\right)\right)}$$
$$\times e^{i\left(\lambda_1 x - \frac{32c_2\lambda_1^2 - 32c_2\nu_2^2 + 15c_1^2 - 64c_2}{64c_2}y - \nu_2 t\right)}.$$

Figure 8 illustrates how the cubic nonlinearity affects the propagation of the fifth solitary wave when $c_2 = 1, \lambda_1 = 0.5, \nu_1 = 1, \nu_2 = 1, t = 0$, and $c_1 = 1,1.25$. There is no doubt that the amplitude of the dark wave increases with increasing the coefficient of cubic nonlinearity.

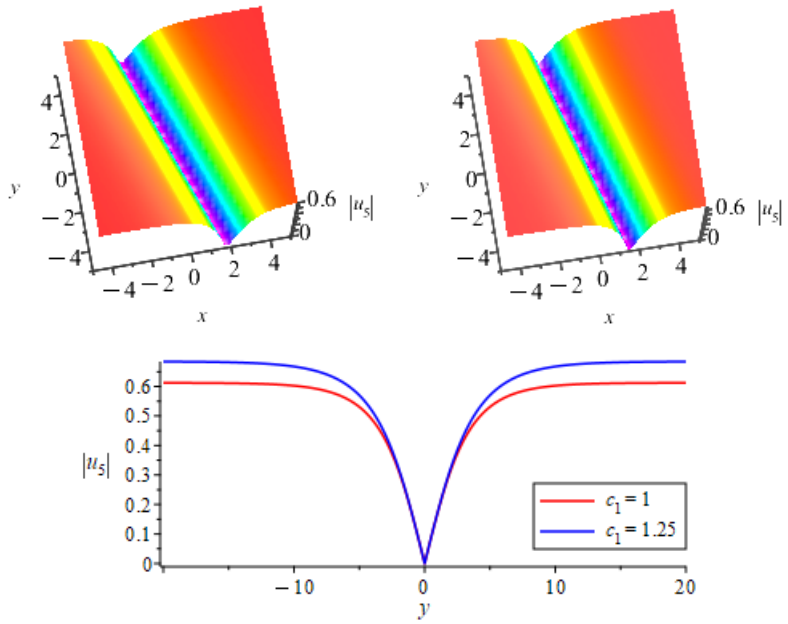

Figure 8: The dark wave in 3D posture for $c_2 = 1, \lambda_1 = 0.5, \nu_1 = 1, \nu_2 = 1, t = 0$, and $c_1 = 1,1.25$; In 2D posture for $c_2 = 1, \lambda_1 = 0.5, \nu_1 = 1, \nu_2 = 1, x = 0, t = 0$, and $c_1 = 1,1.25$

Figure 9 demonstrates an analysis of the impact of quantic nonlinearity on the propagation of the fifth solitary wave when $c_1 = 1, \lambda_1 = 0.5, \nu_1 = 1, \nu_2 = 1, t = 0$, and $c_2 = 1,1.25$. As depicted in Figure 9, the amplitude of the dark wave decreases as the coefficient of quantic nonlinearity increases.

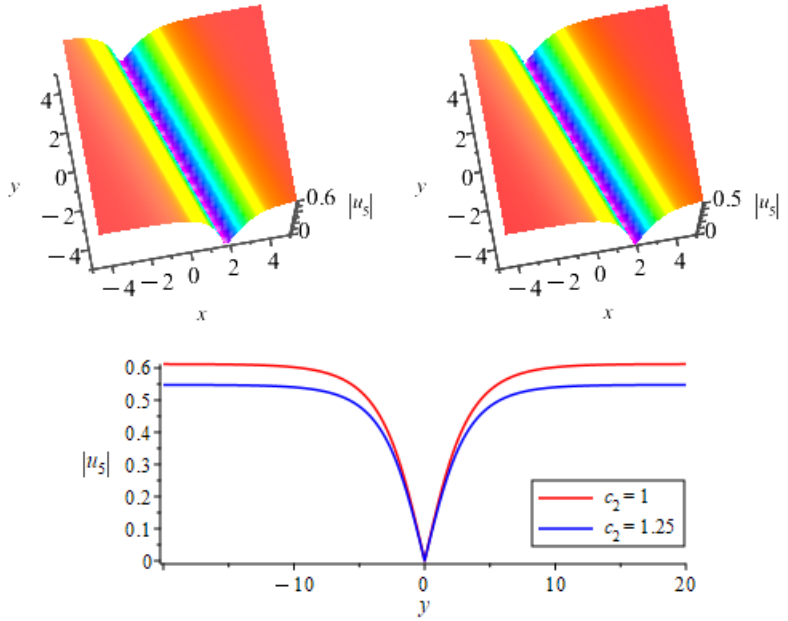

Figure 9: The dark wave in 3D posture for $c_1 = 1, \lambda_1 = 0.5, \nu_1 = 1, \nu_2 = 1, t = 0$, and $c_2 = 1,1.25$; In 2D posture for $c_1 = 1, \lambda_1 = 0.5, \nu_1 = 1, \nu_2 = 1, x = 0, t = 0$, and $c_2 = 1,1.25$

The other solitary waves of the governing model can be derived by considering

$$\psi(\epsilon) = A\left(1 + \frac{\tanh(\epsilon)}{1+\operatorname{sech}(\epsilon)}\right),$$

which A is an unknown, and substituting it into Eq. (9) to find the following algebraic system

$$\frac{1}{4} - \frac{1}{8}\lambda_1^2 + \frac{1}{8}\nu_2^2 - \frac{1}{4}\lambda_2 + A^2c_2 + \frac{1}{2}Ac_1 = 0,$$
$$\frac{1}{4} - \frac{1}{8}\lambda_1^2 + \frac{1}{8}\nu_2^2 - \frac{1}{4}\lambda_2 - \frac{1}{32}\kappa_1^2 + \frac{1}{32}\nu_1^2 + \frac{1}{4}Ac_1 = 0,$$
$$1 - \frac{1}{2}\lambda_1^2 + \frac{1}{2}\nu_2^2 - \lambda_2 - \frac{1}{8}\kappa_1^2 + \frac{1}{8}\nu_1^2 + Ac_1 = 0,$$
$$-\frac{1}{64}\nu_1^2 + \frac{1}{64}\kappa_1^2 - \frac{1}{2}A^2c_2 - \frac{1}{4}Ac_1 = 0.$$

The solutions for the above system are:

$$A = -\frac{3c_1}{8c_2}, \kappa_1 = \pm\sqrt{-\frac{-2c_2\nu_1^2+3c_1^2}{2c_2}}, \lambda_2 = -\frac{8c_2\lambda_1^2-8c_2\nu_2^2+3c_1^2-16c_2}{16c_2}.$$

Therefore, the following solitary waves to the governing equation are derived

$$u_{9,10}(x,t) = \sqrt{-\frac{3c_1}{8c_2}\left(1 + \frac{\tanh\left(\pm\sqrt{-\frac{-2c_2\nu_1^2+3c_1^2}{2c_2}}x + \left(\nu_1\nu_2 \mp \sqrt{-\frac{-2c_2\nu_1^2+3c_1^2}{2c_2}}\lambda_1\right)y - \nu_1 t\right)}{1+\operatorname{sech}\left(\pm\sqrt{-\frac{-2c_2\nu_1^2+3c_1^2}{2c_2}}x + \left(\nu_1\nu_2 \mp \sqrt{-\frac{-2c_2\nu_1^2+3c_1^2}{2c_2}}\lambda_1\right)y - \nu_1 t\right)}\right)}$$
$$\times e^{i\left(\lambda_1 x - \frac{8c_2\lambda_1^2-8c_2\nu_2^2+3c_1^2-16c_2}{16c_2}y - \nu_2 t\right)}.$$

Figure 10 illustrates the evolutionary behavior of the ninth solitary wave for $c_1 = 1.25$, $c_2 = 1$, $\lambda_1 = 0.5$, $\nu_1 = 1$, and $\nu_2 = 1$, when **(a)** $t = -4$, **(b)** $t = 2$, **(c)** $t = 2$, **(d)** $t = 4$.

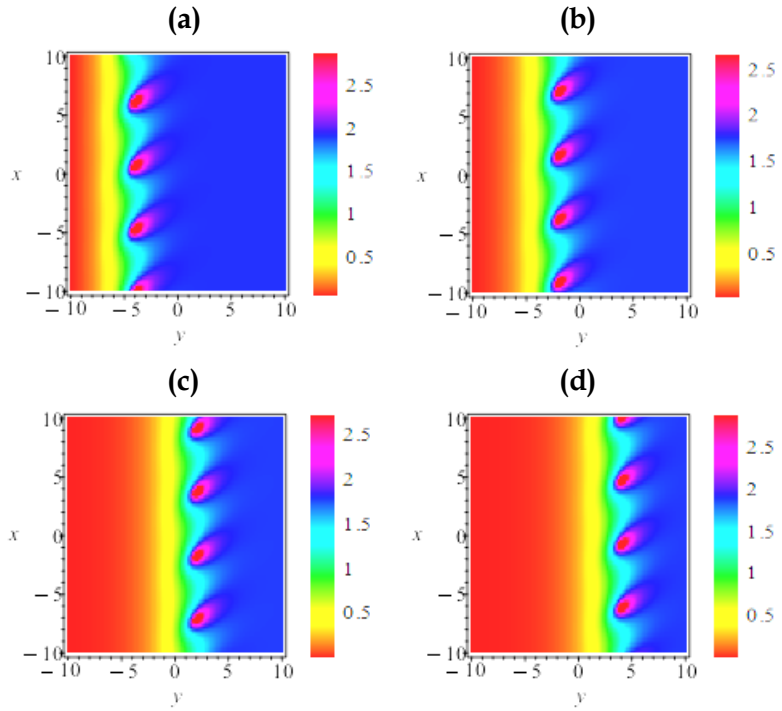

Figure 10: The ninth solitary wave for $c_1 = 1.25$, $c_2 = 1$, $\lambda_1 = 0.5$, $\nu_1 = 1$, $\nu_2 = 1$, and **(a)** $t = -4$, **(b)** $t = 2$, **(c)** $t = 2$, **(d)** $t = 4$

In addition, the authors have analyzed the effect of cubic and quantic nonlinearities on the dynamics of the ninth solitary wave in Figure 11 for

(a): $\{c_1 = 1.25,1.45, c_2 = 1, \lambda_1 = 0.5, \nu_1 = 1, \nu_2 = 1, x = 0, t = 2\}$,

(b): $\{c_1 = 1.25, c_2 = 1,1.2, \lambda_1 = 0.5, \nu_1 = 1, \nu_2 = 1, x = 0, t = 2\}$.

The amplitude of the shock-type wave shows an increasing trend with an increasing coefficient of cubic nonlinearity, as shown in Figure 11**(a)**. From Figure 11**(b)**, it is observed that the amplitude of the shock-type wave decreases with increasing the coefficient of quantic nonlinearity.

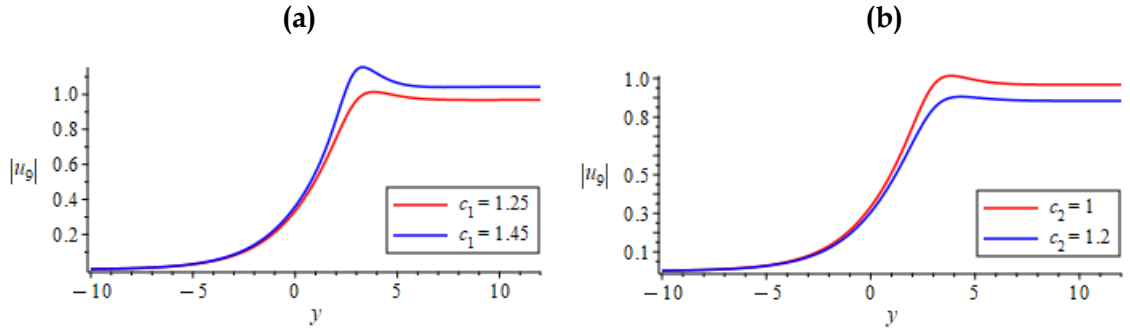

Figure 11: The shock-type wave for **(a)** $c_1 = 1.25,1.45$, $c_2 = 1$, $\lambda_1 = 0.5$, $\nu_1 = 1$, $\nu_2 = 1$, $x = 0$, and $t = 2$; **(b)** $c_1 = 1.25$, $c_2 = 1,1.2$, $\lambda_1 = 0.5$, $\nu_1 = 1$, $\nu_2 = 1$, $x = 0$, and $t = 2$

5. Conclusion

A generalized Schrödinger equation involving the parabolic law of nonlinear refractive index under an external potential was explored extensively in the present paper. A detailed examination of the governing equation for the sideband instability was performed to distinguish the impacts of cubic and quantic nonlinearities on stable and unstable zones. Furthermore, the bifurcation analysis was conducted theoretically and numerically to determine equilibrium points of the generalized Schrödinger equation and identify its periodic and solitary waves. A thorough analysis of the influences of nonlinear effects on the propagation of shock and dark waves modeled by the generalized Schrödinger equation was formally presented. According to the results presented in the present paper, it was observed that 1) The amplitude of shock and dark waves increases with increasing the coefficient of cubic nonlinearity; 2) The amplitude of shock and dark waves shows a decreasing trend with an increasing coefficient of quantic nonlinearity. The future study is to conduct another research on the governing equation and find its other wave patterns using some well-known methods [36–38].

Conflicts of Interest: The authors declare that there are no conflicts of interest regarding the publication of this paper.

References

[1] L. Debnath, Water Waves and the Korteweg–de Vries Equation, in: R. Meyers, (eds) Mathematics of Complexity and Dynamical Systems. Springer, New York, (2012). https://doi.org/10.1007/978-1-4614-1806-1_113.

[2] X. Duan, J. Lu, Y. Ren, R. Ma, The Exact Solutions for the Benjamin–Bona–Mahony Equation, J. Nonlinear Model. Anal. 4 (2022), 628–649. https://doi.org/10.12150/jnma.2022.628.

[3] O.V. Kaptsov, D.O. Kaptsov, Waves and Structures in the Boussinesq Equations, J. Appl. Mech. Tech. Phys. 60 (2019), 377–381. https://doi.org/10.1134/S0021894419020184.

[4] Q. Zhou, D. Yao, F. Chen, Analytical Study of Optical Solitons in Media with Kerr and Parabolic-Law Nonlinearities, J. Mod. Opt. 60 (2013), 1652–1657. https://doi.org/10.1080/09500340.2013.852695.

[5] K. Hosseini, F. Alizadeh, E. Hinçal, M. Ilie, M.S. Osman, Bilinear Bäcklund Transformation, Lax Pair, Painlevé Integrability, and Different Wave Structures of a 3D Generalized KdV Equation, Nonlinear Dyn. 112 (2024), 18397–18411. https://doi.org/10.1007/s11071-024-09944-7.

[6] P. Estévez, Ş. Kuru, J. Negro, L. Nieto, Travelling Wave Solutions of the Generalized Benjamin–Bona–Mahony Equation, Chaos, Solitons Fractals 40 (2009), 2031–2040. https://doi.org/10.1016/j.chaos.2007.09.080.

[7] M. Alquran, R. Alhami, Dynamics and Bidirectional Lumps of the Generalized Boussinesq Equation with Time-Space Dispersion Term: Application of Surface Gravity Waves, J. Ocean. Eng. Sci. (2022). https://doi.org/10.1016/j.joes.2022.05.010.

[8] K. Hosseini, F. Alizadeh, E. Hinçal, B. Kaymakamzade, K. Dehingia, et al., A Generalized Nonlinear Schrödinger Equation with Logarithmic Nonlinearity and Its Gaussian Solitary Wave, Opt. Quantum Electron. 56 (2024), 929. https://doi.org/10.1007/s11082-024-06831-8.

[9] A. Houwe, S. Abbagari, L. Akinyemi, S.Y. Doka, K.T. Crépin, Modulation Instability Gain and Localized Waves in the Modified Frenkel–Kontorova Model with High-Order Nonlinearities, Chaos, Solitons Fractals 173 (2023), 113744. https://doi.org/10.1016/j.chaos.2023.113744.

[10] V.K. Sharma, A. Goyal, J. Goswamy, Study of Modulation Instability for Nonlinear Schrödinger Equation Phase Locked with an External Source, J. Nonlinear Opt. Phys. Mater. 24 (2015), 1550034. https://doi.org/10.1142/S0218863515500344.

[11] Z. Xiong, B. Ren, Plenty of Novel Soliton Molecules and Modulation Instability in the Coherently Coupled Nonlinear Schrödinger Equation, Chin. J. Phys. 90 (2024), 764–772. https://doi.org/10.1016/j.cjph.2024.06.008.

[12] H. Almusawa, M.Y. Almusawa, A. Jhangeer, Z. Hussain, A Comprehensive Study of Dynamical Behavior and Nonlinear Structures of the Modified α Equation, Mathematics 12 (2024), 3809. https://doi.org/10.3390/math12233809.

[13] A. Jhangeer, N. Raza, A. Ejaz, M.H. Rafiq, D. Baleanu, Qualitative Behavior and Variant Soliton Profiles of the Generalized *P*-Type Equation with Its Sensitivity Visualization, Alex. Eng. J. 104 (2024), 292–305. https://doi.org/10.1016/j.aej.2024.06.046.

[14] N. Raza, S.S. Kazmi, G.A. Basendwah, Dynamical Analysis of Solitonic, Quasi-Periodic, Bifurcation and Chaotic Patterns of Landau–Ginzburg–Higgs Model, J. Appl. Anal. Comput. 14 (2024), 197–213. https://doi.org/10.11948/20230137.er.

[15] C. Peng, L. Tang, Z. Li, D. Chen, Qualitative Analysis of Stochastic Schrödinger–Hirota Equation in Birefringent Fibers with Spatiotemporal Dispersion and Parabolic Law Nonlinearity, Results Phys. 51 (2023), 106729. https://doi.org/10.1016/j.rinp.2023.106729.

[16] C. Liu, D. Shi, Z. Li, The Traveling Wave Solution and Dynamics Analysis of the Parabolic Law Nonlinear Stochastic Dispersive Schrödinger–Hirota Equation with Multiplicative White Noise, Results Phys. 54 (2023), 107025. https://doi.org/10.1016/j.rinp.2023.107025.

[17] K. Hosseini, E. Hinçal, F. Alizadeh, D. Baleanu, M.S. Osman, Bifurcation Analysis, Sensitivity Analysis, and Jacobi Elliptic Function Structures to a Generalized Nonlinear Schrödinger Equation, Int. J. Theor. Phys. 63 (2024), 306. https://doi.org/10.1007/s10773-024-05829-y.

[18] N.A. Kudryashov, Method for Finding Highly Dispersive Optical Solitons of Nonlinear Differential Equations, Optik 206 (2020), 163550. https://doi.org/10.1016/j.ijleo.2019.163550.

[19] K. Hosseini, E. Hincal, M. Mirzazadeh, S. Salahshour, O. Obi, et al., A Nonlinear Schrödinger Equation Including the Parabolic Law and Its Dark Solitons, Optik 273 (2023), 170363. https://doi.org/10.1016/j.ijleo.2022.170363.

[20] S. Salahshour, K. Hosseini, M. Mirzazadeh, D. Baleanu, Soliton Structures of a Nonlinear Schrödinger Equation Involving the Parabolic Law, Opt. Quantum Electron. 53 (2021), 672. https://doi.org/10.1007/s11082-021-03325-9.

[21] J.H. He, X.H. Wu, Exp-Function Method for Nonlinear Wave Equations, Chaos, Solitons Fractals 30 (2006), 700–708. https://doi.org/10.1016/j.chaos.2006.03.020.

[22] A.T. Ali, E.R. Hassan, General $\exp_a$–Function Method for Nonlinear Evolution Equations, Appl. Math. Comput. 217 (2010), 451–459. https://doi.org/10.1016/j.amc.2010.06.025.

[23] K. Hosseini, L. Kaur, M. Mirzazadeh, H.M. Baskonus, 1-Soliton Solutions of the (2 + 1)-Dimensional Heisenberg Ferromagnetic Spin Chain Model with the Beta Time Derivative, Opt. Quantum Electron. 53 (2021), 125. https://doi.org/10.1007/s11082-021-02739-9.

[24] H. Triki, A. Pan, Q. Zhou, Pure-Quartic Solitons in Presence of Weak Nonlocality, Phys. Lett. A 459 (2023), 128608. https://doi.org/10.1016/j.physleta.2022.128608.

[25] K. Hosseini, K. Sadri, E. Hinçal, S. Sirisubtawee, M. Mirzazadeh, A Generalized Nonlinear Schrödinger Involving the Weak Nonlocality: Its Jacobi Elliptic Function Solutions and Modulational Instability, Optik 288 (2023), 171176. https://doi.org/10.1016/j.ijleo.2023.171176.

[26] H. Triki, S. Aouadi, C. Wei, Q. Zhou, New Kink-Antikink Solitons of the Pair-Transition-Coupled Nonlinear Schrödinger Equations, Phys. Lett. A 536 (2025), 130290. https://doi.org/10.1016/j.physleta.2025.130290.

[27] K. Hosseini, E. Hincal, F. Mirekhtiary, K. Sadri, O. Obi, et al., A Fourth-Order Nonlinear Schrödinger Equation Involving Power Law and Weak Nonlocality: Its Solitary Waves and Modulational Instability Analysis, Optik 284 (2023), 170927. https://doi.org/10.1016/j.ijleo.2023.170927.

[28] F. Alizadeh, K. Hosseini, S. Sirisubtawee, E. Hincal, Classical and Nonclassical Lie Symmetries, Bifurcation Analysis, and Jacobi Elliptic Function Solutions to a 3d-Modified Nonlinear Wave Equation in Liquid Involving Gas Bubbles, Bound. Value Probl. 2024 (2024), 111. https://doi.org/10.1186/s13661-024-01921-8.

[29] A.I. Aliyu, M. Inc, A. Yusuf, D. Baleanu, Optical Solitary Waves and Conservation Laws to the (2 + 1)-Dimensional Hyperbolic Nonlinear Schrödinger Equation, Mod. Phys. Lett. B 32 (2018), 1850373. https://doi.org/10.1142/S0217984918503736.

[30] E. Tala-Tebue, C. Tetchoka-Manemo, H. Rezazadeh, A. Bekir, Y.M. Chu, Optical Solutions of the (2 + 1)-Dimensional Hyperbolic Nonlinear Schrödinger Equation Using Two Different Methods, Results Phys. 19 (2020), 103514. https://doi.org/10.1016/j.rinp.2020.103514.

[31] D. Baleanu, K. Hosseini, S. Salahshour, K. Sadri, M. Mirzazadeh, et al., The (2 + 1)–Dimensional Hyperbolic Nonlinear Schrödinger Equation and Its Optical Solitons, AIMS Math. 6 (2021), 9568–9581. https://doi.org/10.3934/math.2021556.

[32] H.U. Rehman, M.A. Imran, N. Ullah, A. Akgül, Exact Solutions of (2 + 1)-dimensional Schrödinger's Hyperbolic Equation Using Different Techniques, Numer. Methods Partial. Differ. Equ. 39 (2020), 4575–4594. https://doi.org/10.1002/num.22644.

[33] V. Kumar, R. Jiwari, A.R. Djurayevich, M.U. Khudoyberganov, Hyperbolic (3 + 1)-Dimensional Nonlinear Schrödinger Equation: Lie Symmetry Analysis and Modulation Instability, J. Math. 2022 (2022), 9050272. https://doi.org/10.1155/2022/9050272.

[34] A.M. Wazwaz, M. Abu Hammad, S. El-Tantawy, Bright and Dark Optical Solitons for (3 + 1)-Dimensional Hyperbolic Nonlinear Schrödinger Equation Using a Variety of Distinct Schemes, Optik 270 (2022), 170043. https://doi.org/10.1016/j.ijleo.2022.170043.

[35] K. Hosseini, E. Hinçal, M. Ilie, Bifurcation Analysis, Chaotic Behaviors, Sensitivity Analysis, and Soliton Solutions of a Generalized Schrödinger Equation, Nonlinear Dyn. 111 (2023), 17455–17462. https://doi.org/10.1007/s11071-023-08759-2.

[36] M. Hashemi, A. Haji-Badali, F. Alizadeh, D. Baleanu, Integrability, Invariant and Soliton Solutions of Generalized Kadomtsev–Petviashvili-Modified Equal Width Equation, Optik 139 (2017), 20–30. https://doi.org/10.1016/j.ijleo.2017.03.114.

[37] M.S. Hashemi, A. Haji-Badali, F. Alizadeh, X. Yang, Non-classical Lie Symmetries for Nonlinear Time-fractional Heisenberg Equations, Math. Methods Appl. Sci. 45 (2022), 10010–10026. https://doi.org/10.1002/mma.8353.

[38] A. Hussain, M. Hammad, A.A. Rahimzai, W.S. Koh, I. Khan, Dynamical Analysis and Soliton Solutions of the Space-Time Fractional Kaup–Boussinesq System, Partial. Differ. Equ. Appl. Math. 14 (2025), 101205. https://doi.org/10.1016/j.padiff.2025.101205.